

Thermal oxidation of model molecules to reveal vegetable oil polymerization studied by NMR spectroscopy and self-diffusion

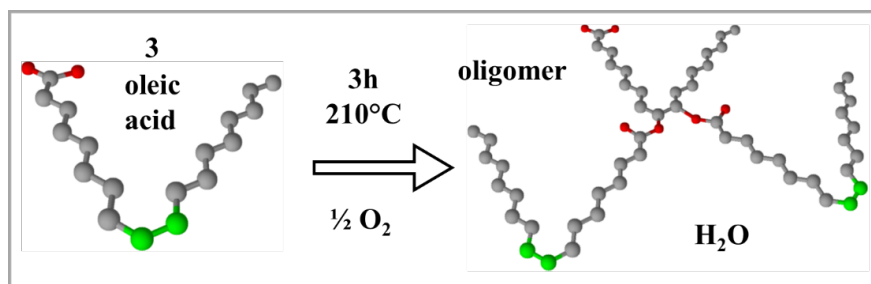
Mara Barani¹, Rino Bonetti¹, and Wallace Parker¹

¹ENI San Donato Milanese Oil and Gas Laboratory

October 20, 2022

Abstract

Oxidative polymerization of plant oils and lipids is poorly understood yet widely encountered. Oil oxidation is accelerated at high temperatures, typically above 110°C, where tri-acylglycerides are converted into toxic compounds and viscous deleterious polymers. Polymerization of mono-unsaturated oil (210°C, 3h, open to air) was investigated by comparing four similar sized molecules with different functional groups: oleic acid, methyl oleate, trans-7-tetradecene and stearic acid. Non-volatile products identified by NMR spectroscopy are minor ketones for saturated fatty acid (stearic acid), epoxides for acyl chains without acid groups (methyl oleate, tetradecane) and copious oligomerization, through ester cross-links, for acyl chains with acid and olefinic groups (oleic acid). Long range C-H coupling clearly shows ester (not ether) cross-links, contradicting long held beliefs. Chain fragmentation also occurs as revealed by species with methylene groups bonded to oxygen, -CH₂-O-C(=O)-R. Large size (slow diffusion) of the first oligomer (trimer) formed by thermal oxidation of oleic acid, (representing hydrolyzed vegetable oil) was evidenced by DOSY (diffusion ordered spectroscopy). Since the first oligomers formed still have reactive groups (olefin, carboxylic acid), poly-ester formation is inevitable at longer oxidation times. Model oil reactions monitored by NMR spectroscopy are important for resolving the complex chemistry of vegetable oil polymerization.



Introduction

Fats and vegetable oils are largely utilized for food and to produce renewable fuels. Conversion of oils to higher molecular weight species (polymerization) during frying or storage is detrimental to health and bio-refinery processes. One measure of edible oil deterioration is polymer concentration. Indeed, vegetable oils also used to synthesize polymers. Yet the molecular transformations and cross-links in the polymers are vague and controversial.

Biodiesel, produced from oils and fats of plants and animals, is a renewable and biodegradable alternative to fossil diesel. Worldwide fossil petroleum reserves are expected to run out this century. Industrial production relies on catalytic transesterification of virgin plant oils (palm, soy, canola) and recycled cooking oils to pro-

duce methyl esters and glycerol byproduct, **Figure 1** . One biorefinery problem is oxidative polymerization reactions , during storage, handling, and conversion, that decrease productivity.

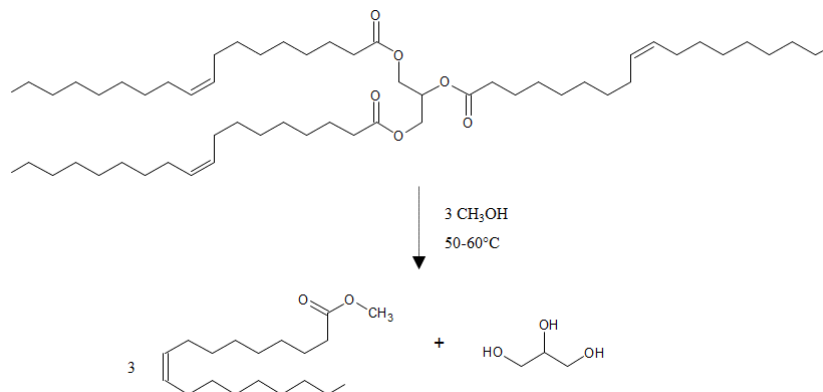


Figure 1. Trans-esterification of triacylglycerol (triolein) to its fatty acid methyl ester (biodiesel) and glycerol.

Oxidation of culinary oils has been studied for decades, detailing the numerous minor species that form (e.g. hydroperoxides, epoxides, aldehydes, acids, ketones) . Multitudes of reports confirm that oxidation and oligomerization occur more rapidly for oils with increased olefinic character. But the oligomers formed during thermal oxidation lack elucidation. Crosslinks in heated oils are usually attributed to C-C bonds without oxygen atmosphere and to ether C-O bonds open to air . Clearly, oxidative polymerization of oil is inconsistent with a Diels-Alder type reaction to give C-C crosslinks . Supposedly, poly-unsaturated “drying oils” (e.g., linseed), used for centuries, polymerize spontaneously in air by ether cross-links .

Clearly, the situation is complex for unsaturated triacylglycerols. Along with ester hydrolysis, glycerol and fatty acids form reactive alkoxy and peroxy radicals which undergo polymerization and scission reactions simultaneously . Molecular size increase during lipid oxidation is easily measured by chromatographic methods. But this gives no cross-link identity

Recently evidence was presented for dispelling ether cross-links in thermally oxidized vegetable oils. Model reactions between carboxylic acids and alcohols (90°C with aeration) showed facile ester formation . NMR spectroscopy found ester bond formation in thermally oxidized oleic acid and soybean oil . Although poorly sensitive, NMR spectroscopy is the most widely utilized spectroscopic technique. It can identify the chemical groups providing the first cross-links and measure molecular size (diffusion rate) of the major products. Information indispensable for unravelling the polymerization reaction.

Due to NMR spectral degeneracy, ester cross-links are difficult to detect starting with tri-acyl glycerides. Hwang et al. had to chromatographically separated the polar fraction of oxidized soybean oil (potatoes frying, 175°C, 24h) to observe ¹³C NMR signals of the new ester species. Also, they observed primary alcohols by ¹H NMR, from fragmentation reactions, in common with our oleic acid oxidation .

We continue simplified stepwise approach to study oil polymerization. This work investigates mono-unsaturated acyl chains (e.g. oleyl) with our standard treatment, 210°C for 3h exposed to air. Oleic acid represents vegetable oil since hydrolysis is an early reaction step. In addition, without NMR signals from acylglycerides and glycerol, spectra are more intense, more resolved, and easier to interpret. Since focus is on characterizing the first larger-sized species formed in polymerization (oligomers), high frying (210°C) above normal frying (175°C), was used for a short time (3h) in open-air containers.

This standard oxidation process is applied to three other “model” molecules (stearic acid, trans-7-tetradecene and methyl oleate) closely related to oleic acid, to evidence the roles of olefinic and carboxylate species in oligomerization. NMR studies provided information on both structures (¹H, ¹³C) and sizes (DOSY) of the

non-volatile molecules produced by auto-oxidation and polymerization. One important structural feature provided by NMR spectroscopy is 3-bond C-H connections which identify the nuclei near the reactive centers (olefin, acid, alcohol) of triacylglycerides.

Results and Discussion

^{13}C NMR spectroscopy identified the main species (above 1% mol C) formed after oxidation open to air (**Table 1**). Light molecular weight species were lost by evaporation with open containers. To verify oligomerization, e.g., formation of larger species, diffusivities of product molecules were measured (**Table 2**). These combined analyses of structure and size reveal the basic aspects of oil oligomerization, which proceed immediately following triglyceride hydrolysis.

NMR spectroscopy is very useful for studying molecules, especially when there is no signal overlap. Thus, the idea of avoiding glycerol-like species. Their role in vegetable oil polymerization will be considered in a subsequent work along with poly-unsaturated oils. ^{13}C NMR spectroscopy quantifies the most abundant species formed, using signals from key chemical groups: carboxylic acid, ester, olefin, glycerol, alkoxy, epoxide, methoxy, methylene and methyl (**Table 1**).

Table 1. Relative amounts of carbon nuclei (% mol)* in model molecules before and after auto-oxidation (210°C, 3h, air) determined by ^{13}C NMR analysis.

| | COOH acid | COOR Ester | -CH= olefin | -CHO- methine O | -C(O)C- epoxide | O-CH ₃ |
|------------------------------------|-----------|------------|-------------|-----------------|-----------------|-------------------|
| stearic acid | 1.0 | - | - | - | - | - |
| stearic acid, 210°C, 3h, air | 0.9 | 0.1 | - | - | - | - |
| 7-tetradecene | - | - | 2.0 | - | - | - |
| 7-tetradecene, 210°C, 3h, air | 0.2 | - | 1.4 | - | 0.4 | - |
| methyl oleate | - | 1.0 | 2.0 | - | - | 1.0 |
| methyl oleate, 210°C, 3h air | 0.3 | 1.4 | 0.1 | - | 0.4 | 1.0 |
| oleic acid | 1.0 | - | 2.0 | - | - | - |
| oleic acid, 210°C, 3h, air | 0.6 | 0.6 | 0.8 | 0.5 | - | - |
| ^{13}C signal shift (ppm) | 180, 178 | 174 | 128-130 | 74 | 57, 59 | 51 |

*) *normalized to 1 or 2 methyl end groups.*

Table 2. Self-diffusion coefficients ($10^{-10}\text{m}^2/\text{s}$) of model molecules before and after oxidation treatment (210°C, 3h, air) determined by ^1H DOSY measurements.

| | D untreated | D unreacted in oxidized products | D major oxidized product | D(untreated)/D(major product) |
|---------------|-------------|----------------------------------|--------------------------|-------------------------------|
| stearic acid | 3.2 | 2.4 | 1.6 | 2.0 |
| 7-tetradecene | 7.8 | 6.2 | 4.8 | 1.6 |
| methyl oleate | 3.5 | 2.6 | 0.7 | 5.0 |
| oleic acid | 1.7 | 0.08 | 0.01 | 170 |

Molecular size was inferred from direct measurements of self-diffusion for species resolved by ^1H DOSY NMR (**table 2**). Often the sizes of oil oxidation products are estimated using size exclusion chromatography in THF solvent, with polystyrene standards. In contrast, DOSY provides self-diffusion coefficients (D) of multiple species in solution resolved by ^1H NMR.

DOSY measures the measured by mean-squared displacement (D), in one direction (z), of a molecule undergoing Brownian motion, over time (t) as $z^2 = 2Dt$. D (in units of m^2/s) is obtained for multiple species

simultaneously, replacing laborious measurements with tracer reagents. Application of a linear magnetic field gradient (G) allows detection of molecular translations (over micrometers), see **Figure S1**. D is used to reveal changes in size. More massive molecules (oligomers) diffuse more slowly. DOSY plots are expanded in the D dimension, leaving out the ^1H signal (at 7.25 ppm) from residual CHCl_3 (in CDCl_3), with fast $D = \text{ca. } 30 \times 10^{-10} \text{ m}^2/\text{s}$.

Stearic acid

Auto-oxidation of stearic acid at 210°C generated minor amounts of ester species giving a ^{13}C signal at 174 ppm, with trace amounts of C-O carbons (65 to 75 ppm signals) and ketone (210 and 42 ppm signals) as shown in **Figure 2**. Since stearic acid is solid at 25°C , it was examined at 50°C (in CDCl_3). ^1H and ^{13}C NMR revealed an average of 17 carbons for this commercial stearic acid used (table 1), due to a smaller (e.g., C_{16}) chain impurity species.

Untreated stearic acid (alone in solution) exhibits one ^1H DOSY signal at $D = (3.2 \pm 0.11) \times 10^{-10} \text{ m}^2/\text{s}$, see **Figure S 2** and **S3**. After oxidation, the D of unreacted stearic acid (present in oxidized product mixture), with methylene ^1H signal at 2.3 ppm (**Figure 3**), is $D = 2.4 \times 10^{-10} \text{ m}^2/\text{s}$, while the minor oxidized species, giving ^1H signals (-CHO-) at 4.0 and 4.9 ppm, diffuses slower at circa $1.6 \times 10^{-10} \text{ m}^2/\text{s}$ (**Figure S4**). Thus, untreated stearic acid diffuses circa two times faster than the major oxidized product containing an ester group (**Table 2**). Minor signals from an ester group are evident at 211 and 42 ppm.

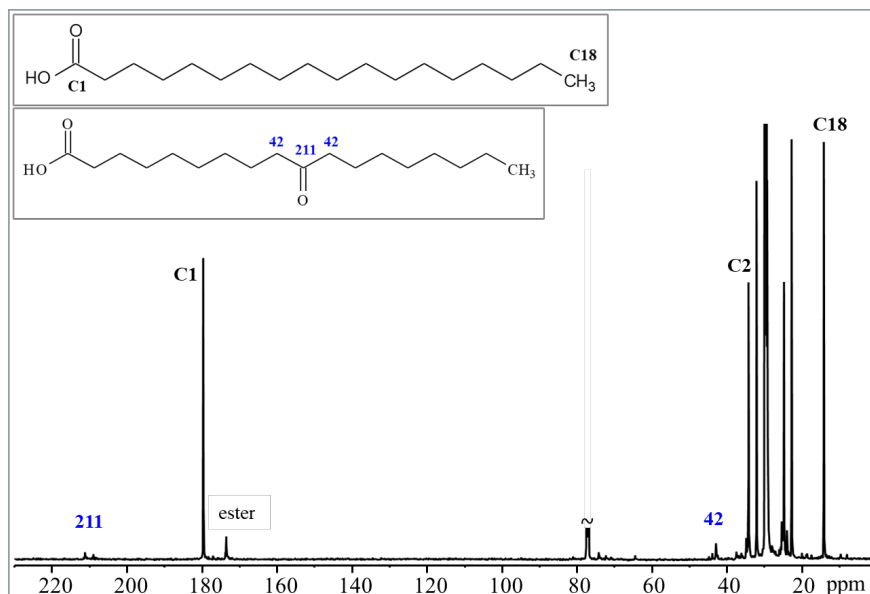


Figure 2: ^{13}C NMR spectrum of thermally treated (210°C , 3h, air) stearic acid dissolved in CDCl_3 (at 50°C).

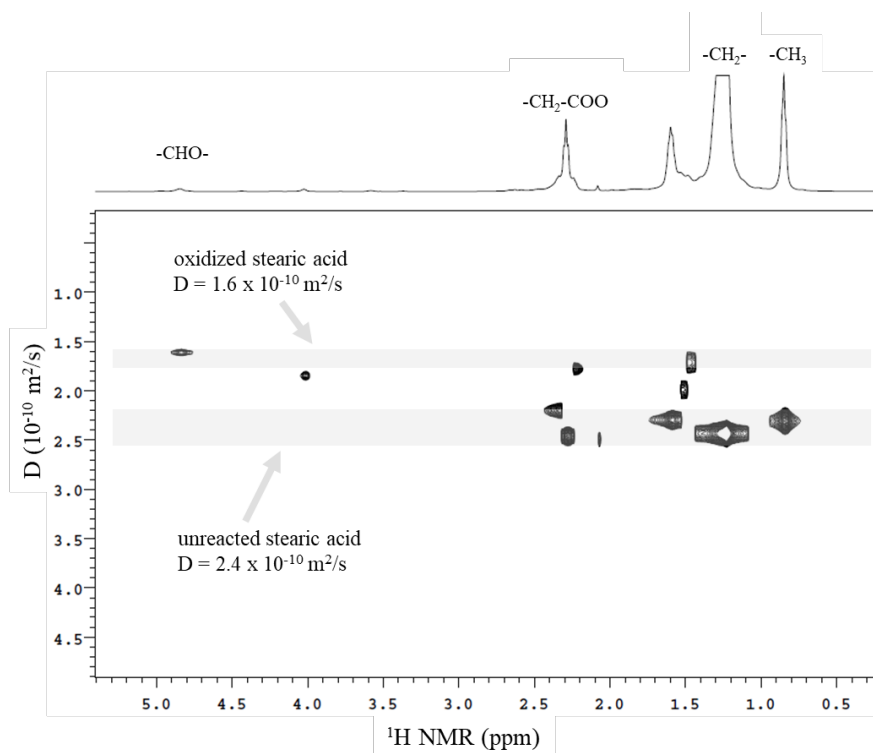


Figure 3: DOSY plot of thermally treated (210°C, 3h, air) stearic acid dissolved in CDCl₃ collected with $\Delta = 140$ ms, $\delta = 5$ ms, $G = 5$ -10k G/cm/DAC in 12 steps.

Trans-7-tetradecene

This molecule was partially transformed (30%) into the corresponding trans-epoxide with ¹³C signals at 59 at 26 ppm (**Figure 4, Table 1**) during auto-oxidation. Clearly the olefin decreased while the epoxide increased. This removes any doubt about the formation of epoxides alpha to the olefin, often proposed in the literature. This observation, based on changes in NMR signal intensities (**Table 1**), was confirmed by HMBC NMR (vide sotto). The methine carbon and hydrogens of the epoxide are not adjacent to an olefin. Thus, if these species form at 210°C, they are short lived intermediates absent in solutions analyzed at 25°C.

Minor ¹³C NMR peaks (between 155 and 215 ppm), from higher oxidized species (aldehyde, ketone, acid) are also present. Transformation of olefinic carbons into carboxylic and aldehyde carbons reveals fragmentation.

DOSY shows no species with largely reduced D compared to untreated trans-7-tetradecene (**Table 2 and Figure S5**) which diffuses at $D = (7.8 \pm 0.1) \times 10^{-10} \text{ m}^2/\text{s}$, **Figure S 7**. After partial oxidation, the trans-7,8-epoxide produced, with its ¹H signal at 2.6 ppm, diffuses somewhat slower $D = (4.8 \pm 0.1) \times 10^{-10} \text{ m}^2/\text{s}$ than unreacted trans-7-tetradecene in the mixture ($6.2 \times 10^{-10} \text{ m}^2/\text{s}$) (**Figure 5**).

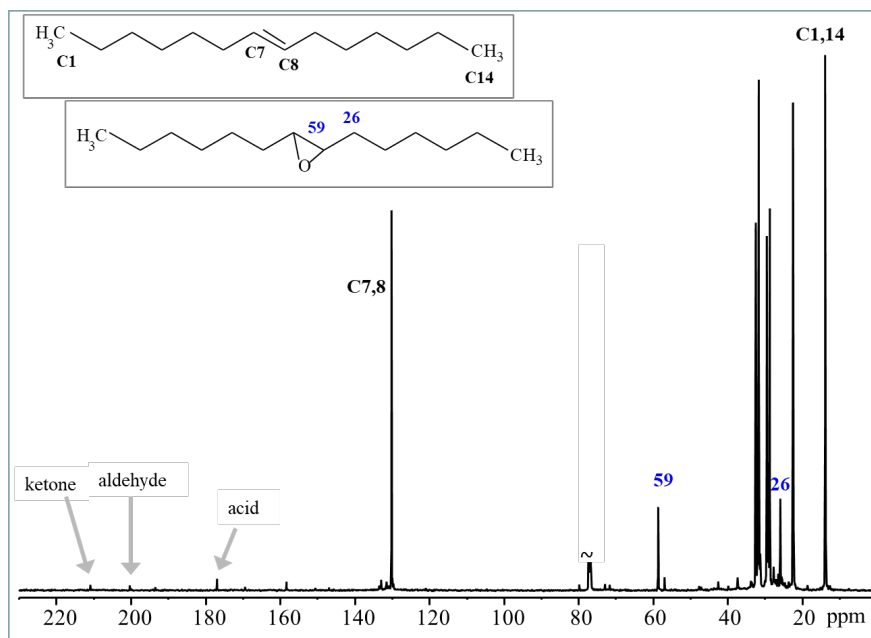


Figure 4: ^{13}C NMR spectrum of thermally treated (210°C, 3h, air) trans-7-tetradecene dissolved in CDCl_3 .

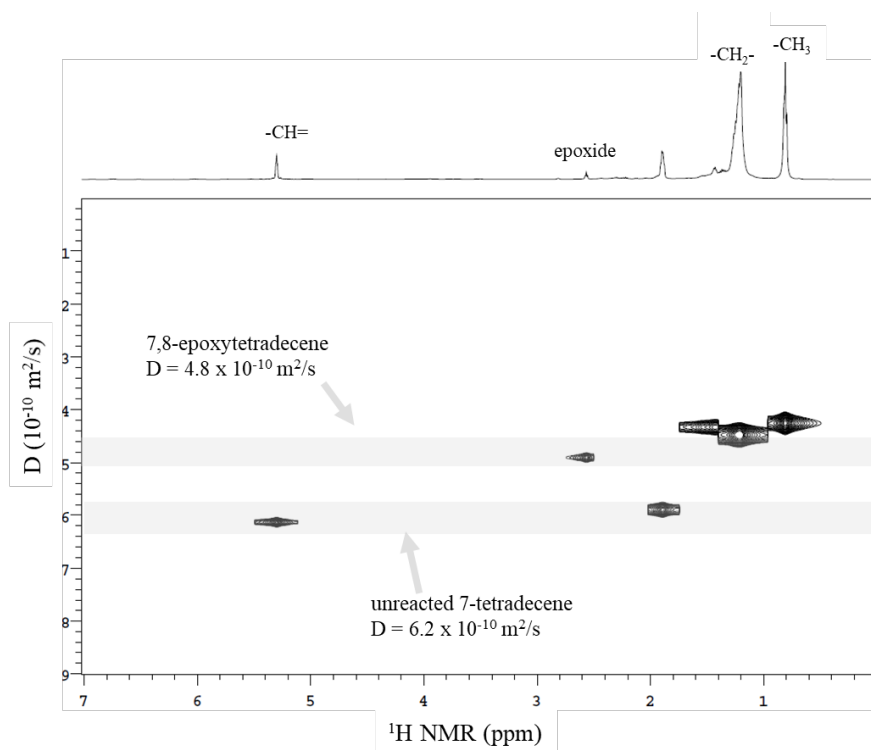


Figure 5: DOSY plot of thermally treated (210°C, 3h, air) trans-7-tetradecene dissolved in CDCl_3 collected with $\Delta = 140$ ms, $\delta = 5$ ms, $G = 5\text{-}10\text{k G/cm/DAC}$ in 12 steps.

Methyl oleate

Thermal oxidation caused a 90% decrease in the olefin¹³C NMR signal (**Figure 6**) of methyl oleate. Olefinic carbons were transformed largely into epoxide, trans (59 ppm) and cis (57 ppm) carbons along with ester, carboxyl and ketone carbons (**Table 1**). Formation of these higher oxidized species also caused an increase in methylene carbons. Thus, one of the olefin carbons was reduced. For example, the CH₂ next to the internal ketone (211 and 42 ppm signals).

Classical reaction schemes for methyloleate oxidation involve unsaturated hydroperoxy species. Molecular structures with double bonds near carbons containing oxygen (peroxy, epoxide or alcohol) can be ruled out based on long-range (HMBC)¹³C-¹H NMR experiments (vide sotto).

DOSY shows untreated methyl oleate with $D = (3.5 \pm 0.1) \times 10^{-10} \text{ m}^2/\text{s}$ (**Table 2** and **Figure S 8**). After oxidation, the small olefinic group (¹H signal at 5.1 ppm) of unreacted methyl-oleate exhibits $D = (1.2 \pm 0.05) \times 10^{-10} \text{ m}^2/\text{s}$ while the abundant newly formed epoxide species (signal at 2.6 ppm) gives $D = (1.0 \pm 0.05) \times 10^{-10} \text{ m}^2/\text{s}$, **Figure 7**. The slowest moving species $D = 0.7 \times 10^{-10} \text{ m}^2/\text{s}$ is associated with the methoxy signal (at 3.2 ppm). However, careful inspection shows a 2-component fit is required (**Figures S9 and S10**), with the slowest component still being circa $D = 0.7 \times 10^{-10} \text{ m}^2/\text{s}$. This component is five times slower than untreated methyl oleate, but only two times slower than unreacted methyl oleate. Thus, as seen above for trans-7-tetradecene, the epoxide (oxidation product) diffuses somewhat slower than the non-oxidized molecule. This is attributed to increased polarity rather than oligomerization.

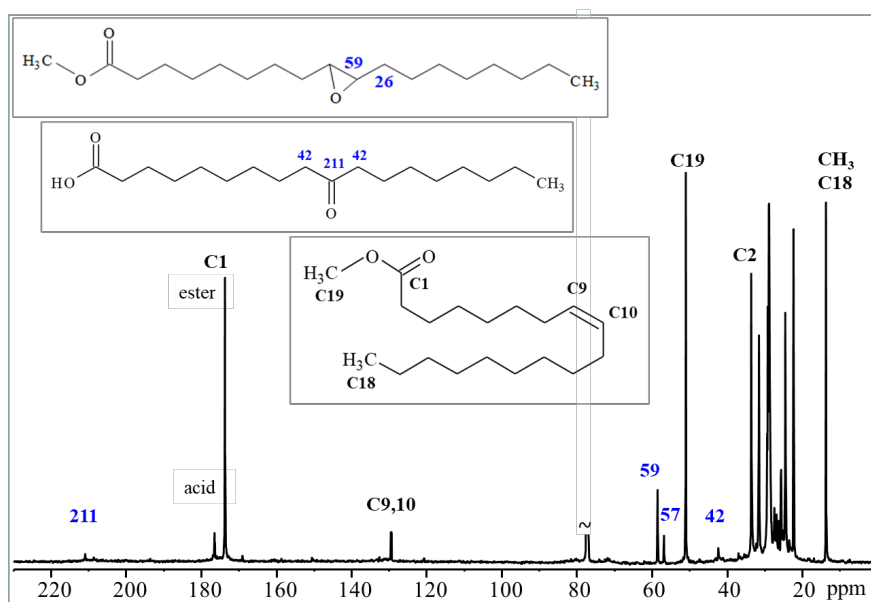


Figure 6: ¹³C NMR spectrum of thermally treated (210°C, 3h, air) methyl oleate dissolved in CDCl₃.

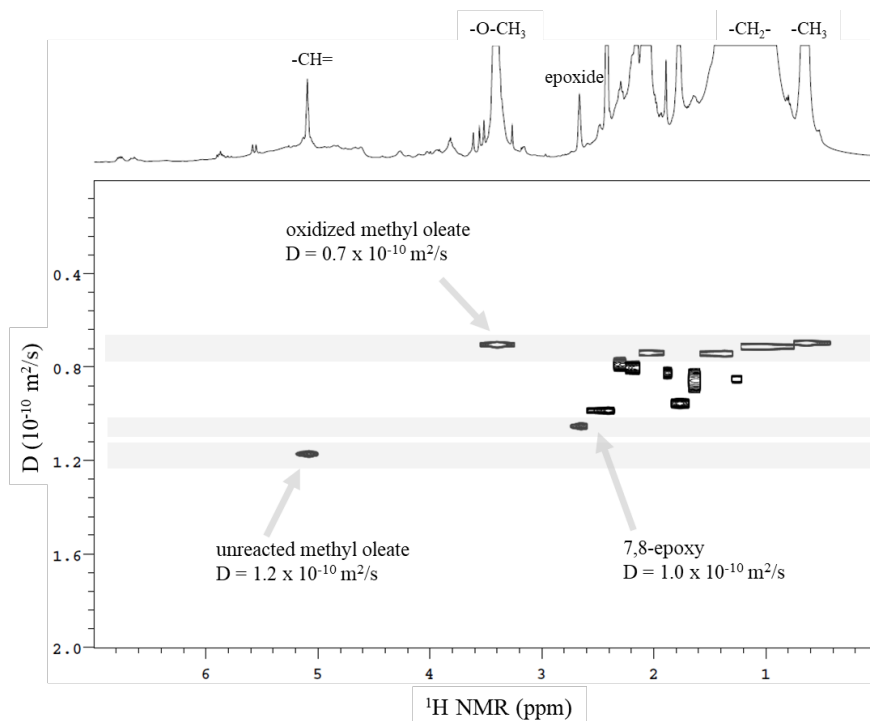


Figure 7: DOSY plot of thermally treated (210°C, 3h, air) methyl oleate dissolved in CDCl_3 collected with $\Delta = 140$ ms, $\delta = 5$ ms, $G = 5\text{-}25\text{k G/cm/DAC}$ in 12 steps and using 1-component fit.

How can unreacted model molecules, in the oxidized mixture, diffuse slower than the untreated one alone? The answer springs from the observation that simple mixtures of model molecules require bi-component DOSY fits. A mixture of untreated model molecules, 7-tetradecene and methyl oleate (in CDCl_3) was examined. Intuition suggests differential diffusion rates will be observed. These molecules are easily distinguished by ^1H NMR spectroscopy, since only 7-tetradecene gives an olefin signal (5.1 ppm) and only methyl oleate gives a methoxy signal (3.5 ppm).

In chloroform these molecules diffuse at the same rate ($5.8 \times 10^{-10} \text{ m}^2/\text{s}$) **Figure S11**, intermediate between faster trans-7-tetradecene ($7.8 \times 10^{-10} \text{ m}^2/\text{s}$) and slower methyl oleate ($3.5 \times 10^{-10} \text{ m}^2/\text{s}$), **Table S 1**. Although these molecules are different (size, polarity), they diffuse at the same rate because of attractive inter-molecular interactions. In fact, CDCl_3 is a “weak” solvent. It is well known that aliphatic chains with polar head groups will associate due to van der Waals forces and the hydrophobic effect. This was confirmed by studying the same mixture in benzene, a solvent able to reduce these forces, and resolve the two species (**Figure S12**). Thus, diffusion of unreacted molecules is slowed (compared to untreated form) due to association with nearby oxidized molecules.

Oleic acid

Auto-oxidation of oleic acid was reported previously. “Clean” observation of a methine carbon bonded to oxygen (-CHO-) drove us to communicate the discovery, **Figure 8**. ^{13}C NMR reveals on average, 40% of the starting carboxylic acid carbons are converted into esters (**Table 1**). Two olefinic carbons and one carboxylic carbon are lost per acyl chain. In correspondence, a major species with one ester per methine bound to oxygen (CHO-) forms (T1 below). Previously, a dimer was suggested. But, to satisfy overall oxidation, addition of oxygen to both olefinic carbons (C9,10) is required. Otherwise, with only one ester bond (mono-acylation), net oxidation does not occur (**Figure S13**).

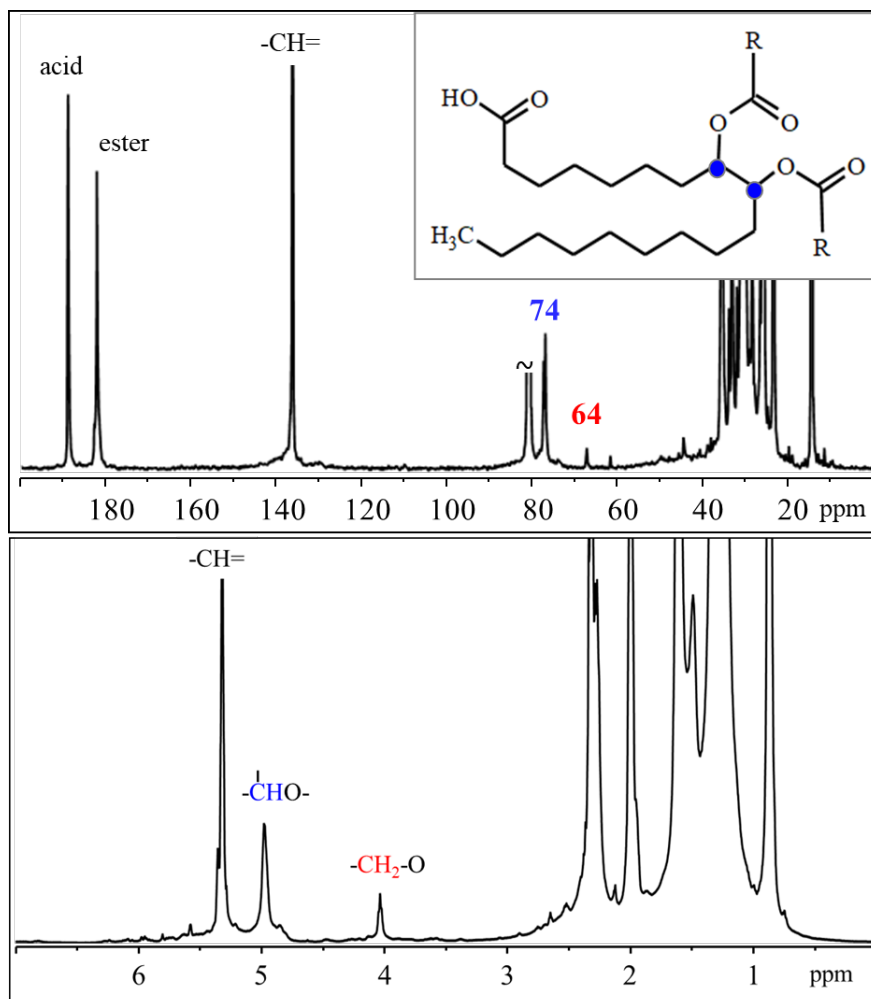


Figure 8: ^1H (bottom) and ^{13}C (top) NMR spectra of thermally treated (210°C, 3h, air) oleic acid dissolved in CDCl_3 expanded vertically to evidence signals from major (blue) oxidation product with CH-O (74 ppm, ^{13}C and 4.0 ppm, ^1H) signals and the minor (red) oxidation products. (insert, R = $\text{C}_{17}\text{H}_{34}$)

Untreated oleic acid, dissolved in CDCl_3 , diffuses with $D = (1.7 \pm 0.1) \times 10^{-10} \text{ m}^2/\text{s}$, **Figure S 12**. After oxidation, two distinct components: $D = 0.01 \times 10^{-10} \text{ m}^2/\text{s}$ and $D = 0.08 \times 10^{-10} \text{ m}^2/\text{s}$ were observed, **Figure 9 and S15**. The slowest component, more than a hundred times slower than untreated oleic (**table 2**), reveals a dramatic increase in molecular size.

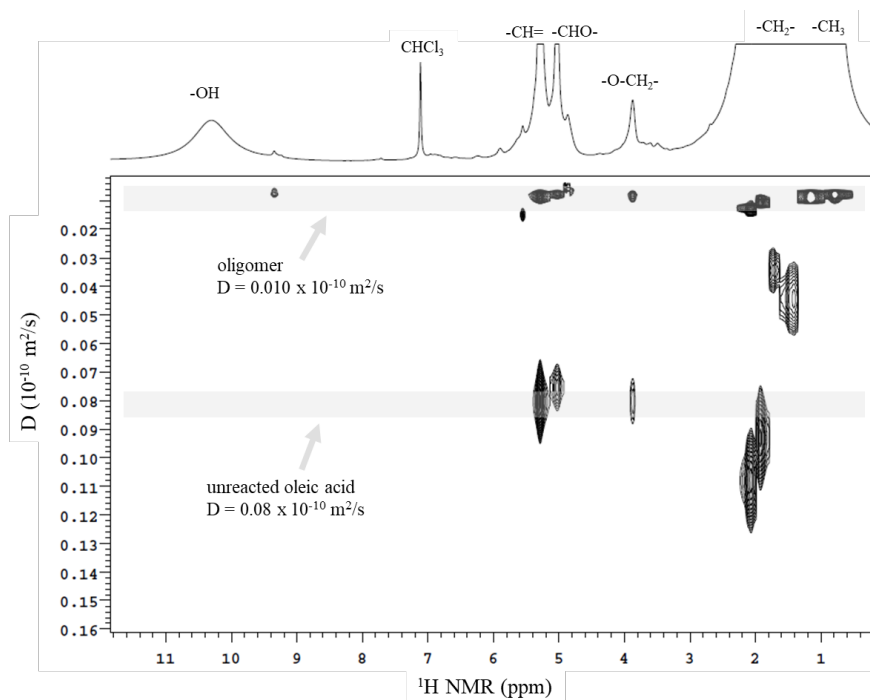


Figure 9: DOSY plot of thermally treated (210°C, 3h, air) oleic acid dissolved in CDCl_3 collected with $\Delta = 90$ ms, $\delta = 40$ ms, $G = 5\text{-}25\text{ k G/cm/DAC}$ in 15 steps using 2-component fit. Signal near 10 ppm, from an acidic H, does not exhibit a cross-peak because of rapid transverse relaxation.

Oligomers and acid fragments

The major oxidation product of oleic acid gives a methine carbon bonded to oxygen with ^{13}C and ^1H signals at 74 and 4.9 ppm, respectively. In addition, we know the hydrogen of this methine group is three-bonds away from the carboxylate carbon of the ester group (**supplementary information** ref). Thus, the methine bonded to oxygen is not an ether. This information, combined with the size increase found by DOSY, allows the oligomerization mechanism to be hypothesized.

Initially, in theory, oxidation of oleic acid can produce several types of “monomeric” species (M1-M3, **Figure 10**, neglecting peroxy species). However, NMR shows none of these species (M1-M3) are present in large amounts (**Figure 8**). M1, with its methine (CH-O) carbon giving a ^{13}C signal at 67 ppm, is missing. No epoxide ^{13}C signals (57, 59 ppm) for M2 were observed. M3 is not present either since there is no ^1H methine CH-O signal at 3.5 ppm (**Figure S16**). Thus, the monomeric oxidation product of oleic acid is reactive and was consumed before NMR observation. Also, hydroperoxy species, which give ^{13}C signals near 80 ppm (**Figure S17**), were not observed.

It is important to note that M1 type species (alpha-hydroxy olefin), widely accepted oxidation products in the literature, were not observed. Such chemical groups are easily distinguished using $2\text{D }^{13}\text{C}\text{-}^1\text{H}$ HMBC NMR spectroscopy. This inverse detection method reveals “long range” scalar coupling between hydrogens and carbon nuclei 3 bonds away. The olefinic hydrogens in all samples studied here do not exhibit correlations with carbons bonded to oxygen (e.g. **Figure S18**).

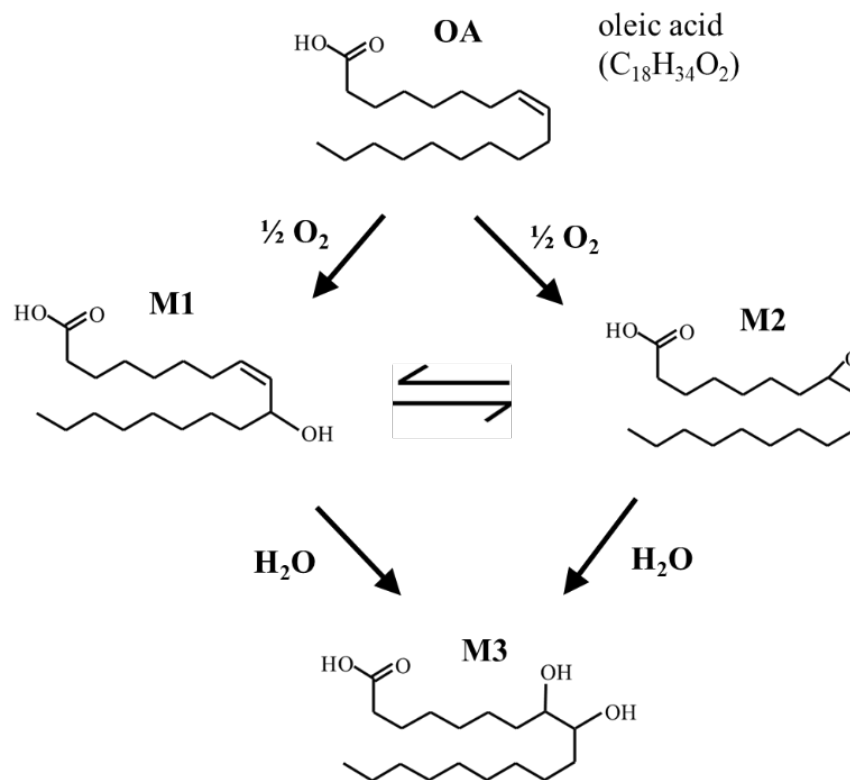


Figure 10. Oxidization of oleic acid to produce monomeric species, without considering peroxy species.

The first potential oligomer (**Figure 11**), dimer D1 (mono-ester) formed by ring-opening mono-acylation of epoxide M2, was not observed (**Figure S19**). However, species T1, the di-acylated epoxide is consistent with the spectral observations. Presumably, D1 was not present in the oxidized products because it quickly reacts with oleic acid or oxygen to form T1 or fragments (F1, F2). Trimer T1, or even a larger species, is also consistent with DOSY measurements. The oligomer formed by thermal oxidation of oleic acid diffuses eight times slower than extra-virgin olive oil ($D = 0.082 \times 10^{-10} \text{m}^2/\text{s}$) **Table S1**, a tri-acylglycerol (885 g/mol) three times heavier than oleic acid (282 g/mol).

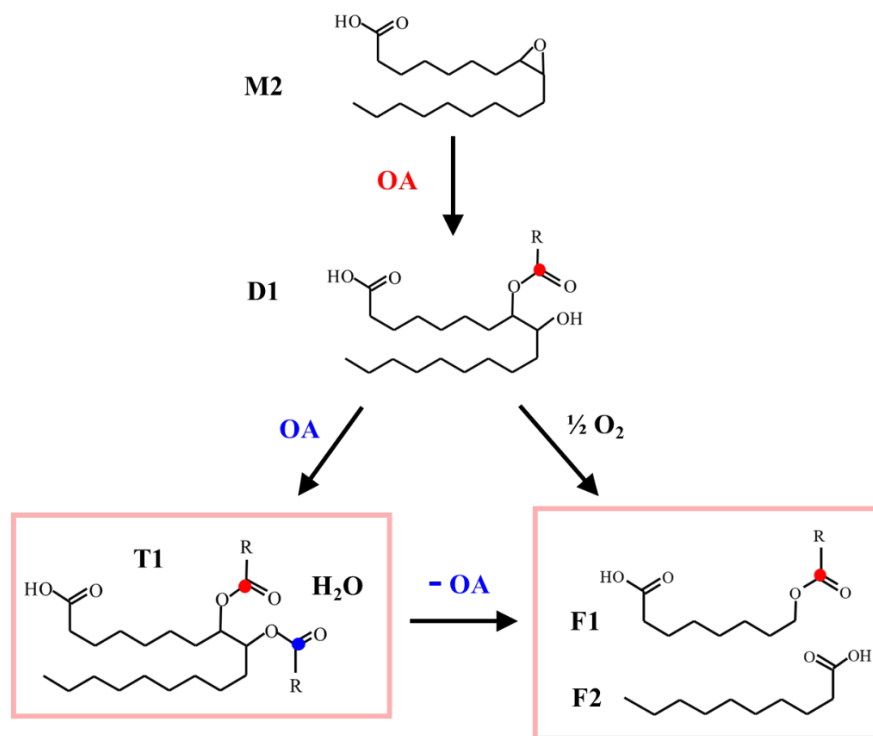


Figure 11. Oligomerization and fragmentation reactions for oxidized oleic acid consistent with observation of trimer T1 and fragments F1, F2 by NMR spectroscopy. OA = oleic acid, R = C₁₇H₃₄.

Reaction of D1 with oleic acid to give T1 (Figure 11) corresponds to the rapid reaction of an alcohol with a carboxylic acid described by Ball et al. . The minor oxidized species contains F1, with a methylene carbon attached to oxygen (CH₂-O) gives¹³C and ¹H signals at 68 and 4.0 ppm, respectively. A methylene bonded to oxygen (CH₂-O) does not exist in oleic acid. This paramount finding could be easily missed starting with acylglycerols, since they have these carbon types. Formation of such a chemical group, stemming from a primary alcohol, can only result from cleavage.

Fragment F1 is rarely proposed in the literature (e.g. Figure S20), which instead claims F2. Note that oxidative cleavage of epoxide M2 to give a primary alcohol does not occur since it would exhibit a ¹H CH₂-O signal at 3.5 ppm. Instead, a ¹H CH₂-O signal was observed at 4.0 ppm (Figure 8).

Conclusions

Experiments with four model molecules (stearic acid, trans-7-tetradecene, methyl oleate and oleic acid) under high frying thermal oxidation (210°C, 3h, in air) demonstrated that oxidative polymerization predominates only when there are olefin and carboxylic acid functions on the *same* molecule. Oleic acid is thus an ideal model molecule for investigating the initial polymerization events in vegetable oil.

NMR spectroscopy experiments identified the first major (non-volatile) thermal oxidation products generated. Under our oxidation conditions, with model molecules, we evidenced: stearic acid forms a bit of internal ester, trans-7-tetradecene forms (30%) epoxide, methyl oleate largely forms (90%) epoxide and oxidized monomers while oleic acid forms (40%) much larger species and fragments. Changes in NMR signal intensities reveal oxidation occurs at the double bond. Long-range¹³C-¹H correlation experiments confirm there are no species with oxygen near a double bond.

Monomeric epoxide species (M2), formed first during oxidation of oleic acid at 210°C, undergo rapid diacylation through inter-molecular ester cross-links (T1 in Figure 11). Fragmentation of oleic acid during

oxidation was revealed by formation of methylene groups bonded to oxygen ($\text{CH}_2\text{-O}$). Observation of these unprecedented fragments ($\text{CH}_2\text{-O}$ rather than $\text{CH}_2\text{-C(O)O}$) along with the di-ester trimer demonstrate experimentally the first steps in vegetable oil polymerization.

Ester cross-links are seldom contemplated in vegetable oil polymers. Drying and poly-unsaturated oils are thought to increase molecular size by ether cross-links. Here we show, for a mono-unsaturated oil, the reactive olefinic groups form epoxides which then cross-link through ester groups. Surprisingly, this knowledge, from experimental NMR observations and model chemical reactions, is being realized only now. The first trimer formed for oleic acid is still reactive since it possesses both oleic and carboxylic acid functions. This allows propagation of deleterious polyesters at longer reaction times.

Facile formation of polyesters provides a new perspective on oxidation of lipids and vegetable oils. This report dispels traditional, widely accepted, reaction schemes involving ether cross-links and hydroxy-olefin species.

Experimental

Four model molecules: methyl oleate, trans-7-tetradecene, oleic acid and stearic acid were purchased from Fluka Aldrich. Each substance was studied pure (dissolved in CDCl_3) and after oxidation at 210°C for 3 hours in containers open to air with stirring as previously.

NMR samples were prepared by dissolving 60 mg of substance in 60 mg of CDCl_3 and contained in 5 mm tubes. NMR spectra were collected with a 12 Tesla Varian-500 spectrometer. Quantitative ^{13}C observation at 125 MHz was made with 300 ppm spectral window, 30° pulse (3.2 μs), inverse-gated ^1H decoupling during 0.7 s acquisition time, 12 s relaxation delay and 128 to 2 k repetitions. ^1H observation at 500 MHz was made with 20 ppm spectral window, 40° pulse (6.0 μs), acquisition time of 0.8 s, relaxation delay of 10 s and 12 repetitions. Chemical shifts are referenced to TMS (tetramethylsilane) at 0 ppm using the solvent signal as secondary reference: ^1H (CHCl_3 at 7.25 ppm) ^{13}C (CDCl_3 triplet centered at 77.0 ppm).

A standard composed of $\text{H}_2\text{O-D}_2\text{O}$ (1:1 vol), with known D ($2.1 \times 10^{-9} \text{ m}^2/\text{s}$ at 25°C) was used to calibrate the gradient strength and confirm reproducible measurements. G_{cal} value = 0.00190 G/cm/DAC. Our D values are consistent with others (**Table S1**). DOSY parameters are reported in figure captions. Big delta (observation time) was usually fixed at 140 ms. Small delta (pulsed gradient time) was also fixed but choosing it (from 2 to 30 ms) to realize a full change in echo intensity given the arrayed gradient strengths (G) incremented as detailed in **Supporting Information**. “Doneshot” was used in all cases except for thermally treated stearic acid studied at 50°C . Convection correction was applied in this case using Varian’s “Dbppstecc” pulse sequence.

Since D is concentration dependent, we reason in terms of relative values (large changes) in D . Pure model molecules, dissolved in CDCl_3 , exhibited single D values. Oxidized oil molecules did not always exhibit mono-exponential behavior in chloroform, due to inter-molecular attractive interactions. This also slowed the diffusion of unreacted molecules in oxidized solutions.

Supporting information

Thermal oxidation of model molecules to reveal vegetable oil polymerization studied by NMR spectroscopy and self-diffusion

M. Barani, R. Bonetti, W. Parker

Physical Chemistry Department, Eni, San Donato (MI), Italy

Table S 1: Self-diffusion coefficients (D) of untreated model molecules (at 25°C , except stearic acid) determined by pulsed-field gradient and DOSY NMR spectroscopy.

| molecule | solvent | D ($10^{-10} \text{ m}^2/\text{s}$) | ref |
|-------------------------------------|-----------------|---|-----------|
| stearic acid (50°C) | CDCl_3 | 3.2 | this work |

| molecule | solvent | D (10^{-10} m ² /s) | ref |
|--------------------------------|---------|-----------------------------------|------------------|
| stearic acid (50°C) | none | 1.9 | Iwahashi et al. |
| octanoic acid | CCl4 | 3.0 | Matsuzawa et al. |
| trans-7-tetradecene | CDC13 | 7.8 | this work |
| n-tetradecane | none | 5.2 | Mills |
| methyl oleate | CDC13 | 3.5 | this work |
| methyl oleate | none | 3.0 | Meiri et al. |
| trans-7-decene + methyl oleate | CDC13 | 5.8 | this work |
| oleic acid | CDC13 | 1.7 | this work |
| cis-11-octadecenoic acid | none | 0.6 | Iwahashi et al. |
| extra-virgin olive oil | none | 0.082 | Ancora et al. |

¹H DOSY

Following the suggestion of Socha , analytical limitations of 1D¹H NMR applied to plant oils were circumvented using diffusion-ordered NMR spectroscopy (DOSY) . DOSY is a widely used pulsed field gradient NMR technique that separates species according to their diffusion coefficient (D) .

Oil undergoes hydrolysis, oxidation, and polymerization during heat treatment, resulting in the formation of compounds that have a higher molecular weight and higher polarity than normal unaltered triacylglycerols. Higher molecular-weight compounds diffuse more slowly than those of lower molecular weight and therefore DOSY can easily differentiate them.

In the origin method to measure D, of Stejskal and Tanner in 1965, a Hahn spin echo sequence is used with insertion of two linear magnetic field gradient pulses (G), of δ duration and separated by delay Δ , during the echo periods (**Figure S1**). At the beginning of the experiment the net magnetization is oriented along the z axis and the 90° pulse rotates the magnetization in the reading plane x-y. At time t, a pulse gradient of δ duration and G magnitude is applied (in the z direction) to encode the position of nuclei in the sample. After t again, a 180° pulse and another pulse gradient of the same duration and magnitude of the previous are applied to decode positions of nuclei. Without diffusion the echo signal is maximum. Movement of magnetic hydrogen nuclei causes echo attenuation. Faster diffusion (molecular translation) causes greater attenuation of the echo signal collected.

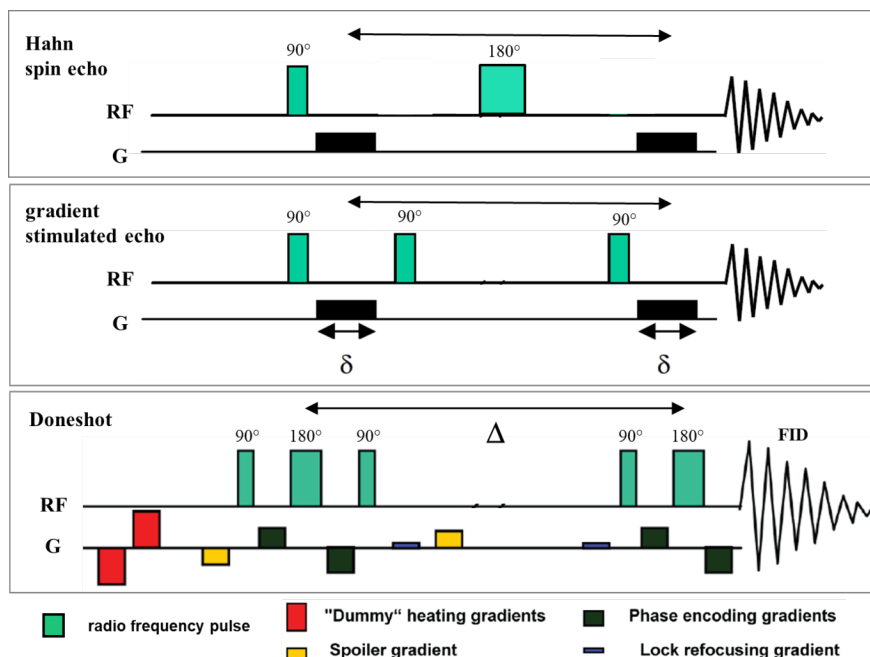


Figure S 1: Hahn spin echo (top), gradient stimulated echo (middle) and Doneshot (bottom) pulse sequences, adapted from VnmrJ Liquids NMR User Guide (Varian).

“Oneshot” pulse sequence used here is based on the stimulated echo sequence, *Errore. L’origine riferimento non è stata trovata.* This sequence allows longer diffusion times (Δ) than for the original spin echo method, facilitating detection of hydrogens with short transverse relaxation times. It acquires one transient per gradient level and uses unbalanced bipolar pulse pairs and spoiler gradients to improve performance.

The observation time for diffusion (Δ) and gradient duration (δ) duration are kept constant. This removes any contribution from relaxation. Decay in intensity (I) of each ^1H signal as G strength increases is fit to the Stejskal-Tanner equation (Eq. 1).

$$I(G) = I(0) \cdot \exp \left[-D (\gamma G \delta)^2 \left(-\frac{\delta}{3} \right) \right] \quad \text{Eq. 1}$$

Curve fitting gives the self-diffusion coefficient (D) as the other parameters are known (γ = gyromagnetic ratio = $4.258 \times 10^3 \text{ s}^{-1} \text{ G}^{-1}$). DOSY plots are processed in 2D through a Laplace transform. The 2D presentation has diffusion coefficients D along the y-axis and chemical shift along the x-axis (**Figure S2**).

Diffusion of $\text{D}_2\text{O}:\text{H}_2\text{O}$ (1:1 v/v) standard with known D ($2.1 \times 10^{-9} \text{ m}^2/\text{s}$ at 25°C) was routinely examined to calibrate G and ensure reproducible experimental conditions, G_{cal} value = 0.00190 G/cm/DAC . DOSY observation time (Δ) was fixed, usually at 140 ms. Plots of echo intensity I (y-axis) versus the gradient area squared $(\gamma G_z \delta)^2 ([?]-\delta/3)$ in ns/m^2 (x axis) yielded D , **Figure S3**.

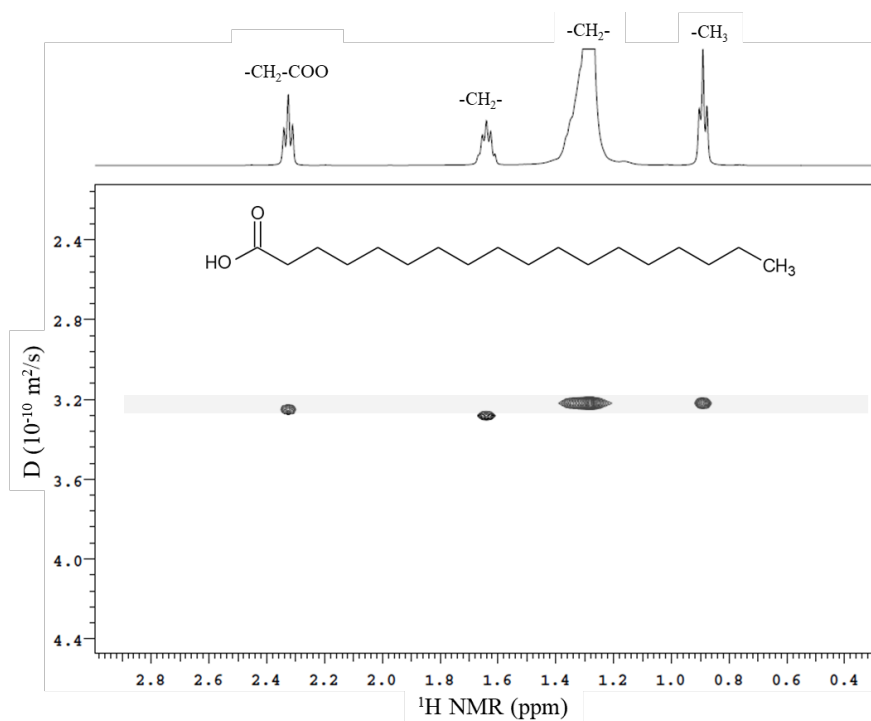


Figure S 2: DOSY plot of untreated stearic acid dissolved in CDCl_3 (at 50°C) collected with $\Delta = 140$ ms, $\delta = 5$ ms, $G = 5\text{-}13\text{ k G/cm/DAC}$ in 15 steps.

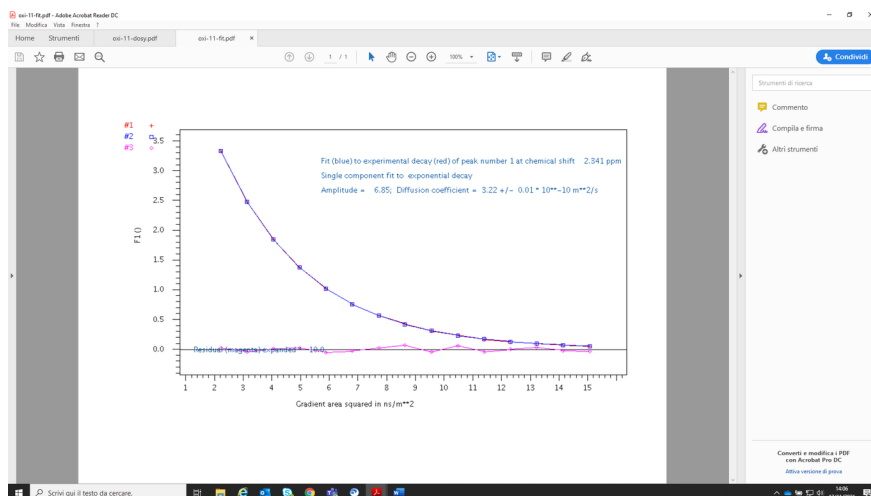


Figure S 3: Plot of echo intensity I (y axis) versus the gradient area squared $(\gamma G_z \delta)^2 ([?] - \delta/3)$ in ns/m^2 (x axis) for ^1H NMR peak at 2.3 ppm of untreated stearic acid (at 50°C).

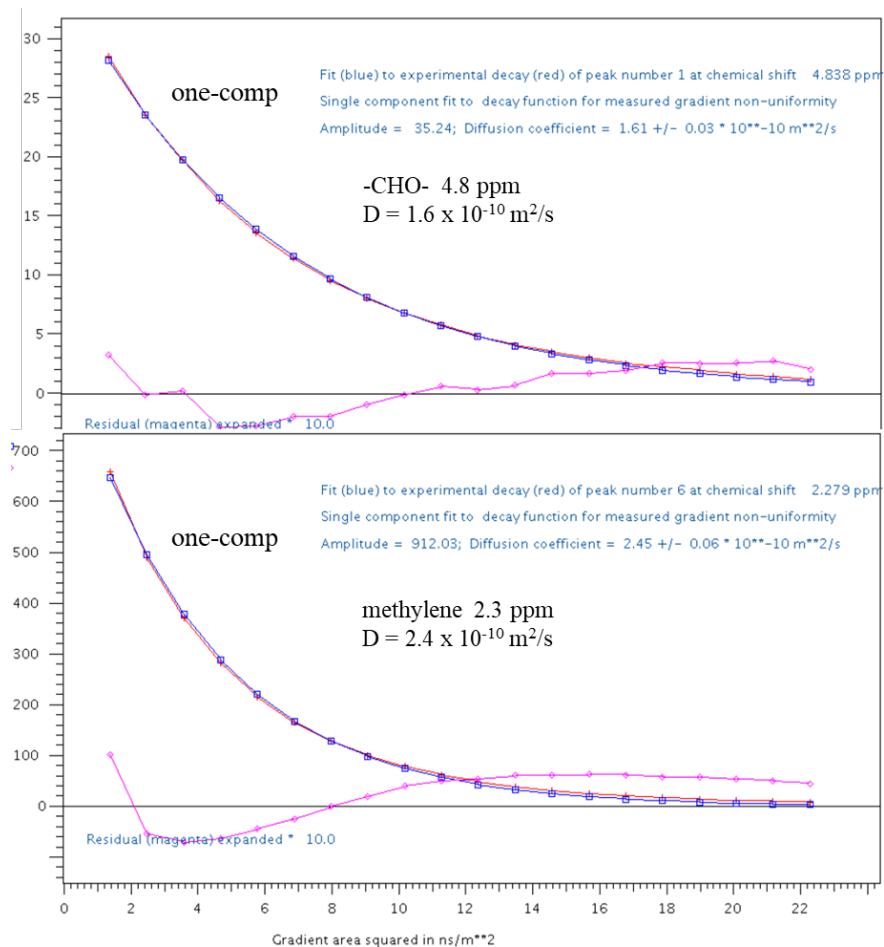


Figure S 4: Plot of echo intensity I (y axis) versus the gradient area squared $(\gamma G_z \delta)^2 ([?] - \delta/3)$ in ns/m^2 (x axis) for ^1H NMR peaks at 2.3 and 4.8 ppm of thermally treated (210°C , 3h, air) stearic acid.

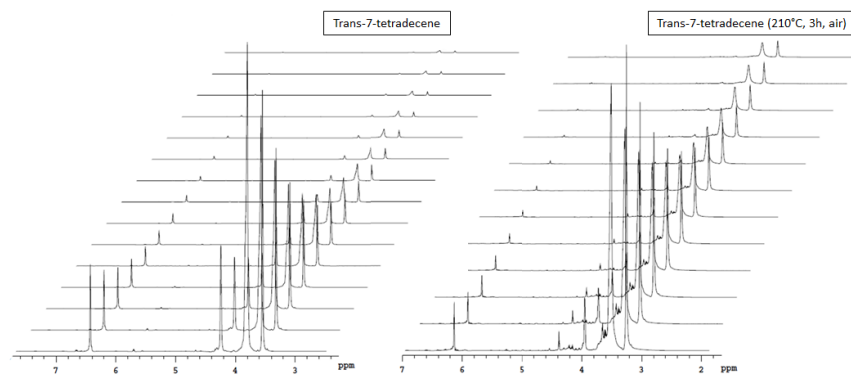


Figure S 5: ^1H NMR intensity as a function of applied magnetic field gradient strength (5-10k G/cm/DAC in 12 steps) used to calculate D for trans-7-tetradecene before and after thermal treatment.

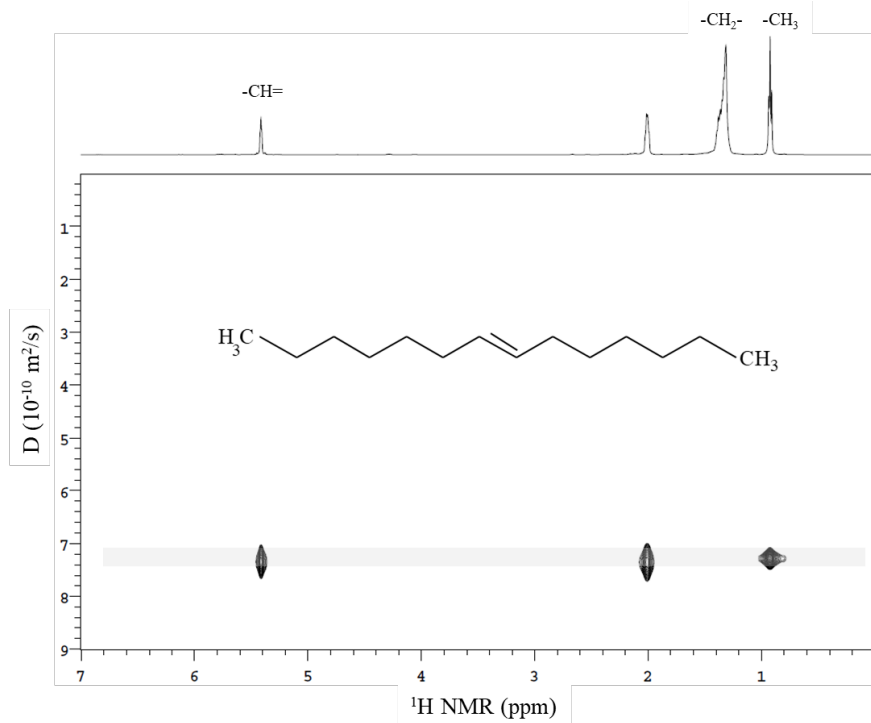


Figure S 6: DOSY plot of untreated trans-7-tetradecene dissolved in CDCl_3 collected with $\Delta = 140$ ms, $\delta = 5$ ms, $G = 5\text{-}10\text{ k G/cm/DAC}$ in 12 steps.

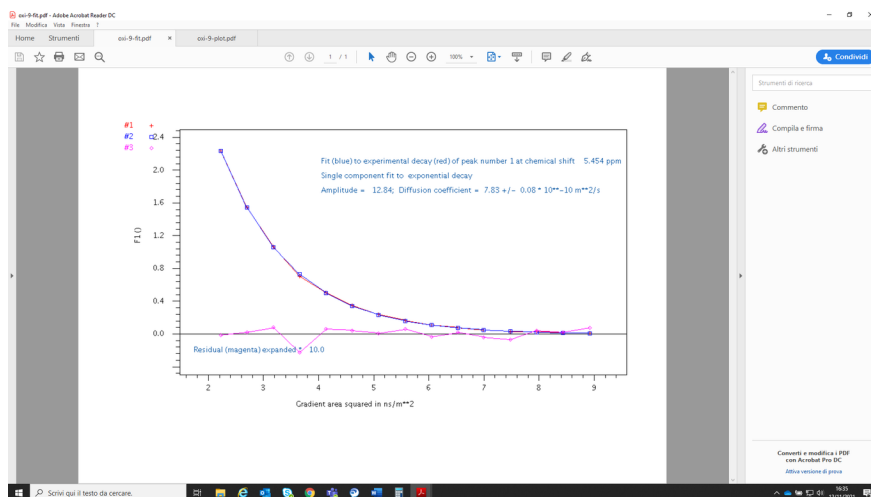


Figure S 7: Plot of echo intensity I (y axis) versus the gradient area squared $(\gamma G_z \delta)^2 ([?] - \delta/3)$ in ns/m^2 (x axis) for ^1H NMR peak at 5.5 ppm of untreated trans-7-tetradecene.

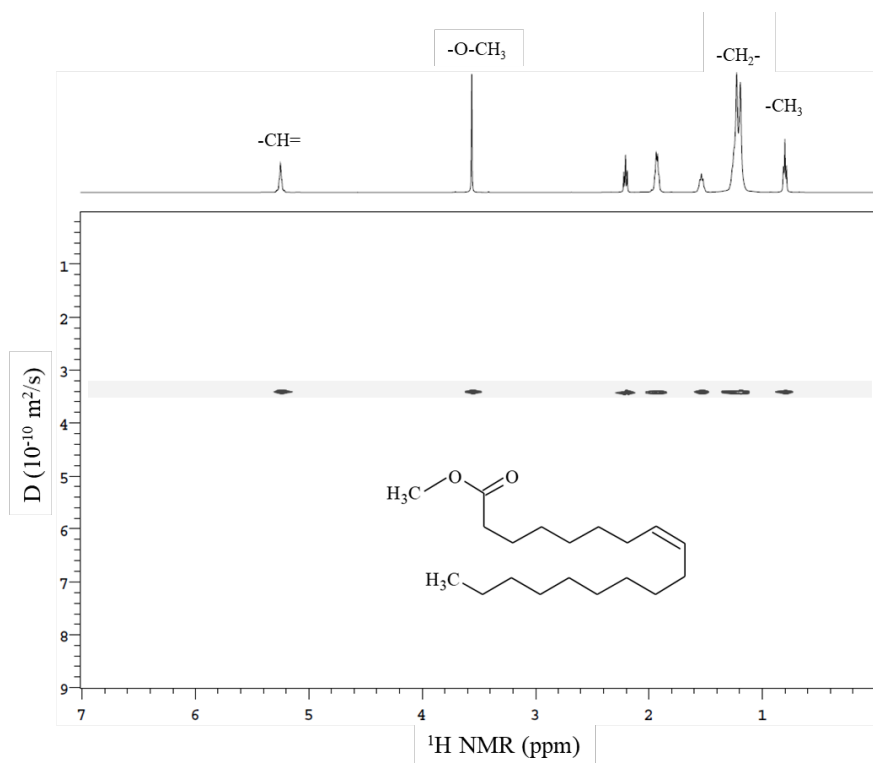


Figure S 8: DOSY plot of untreated methyl oleate dissolved in CDCl_3 collected with $\Delta = 140 \text{ ms}$, $\delta = 5 \text{ ms}$, $G = 5\text{-}10\text{k G/cm/DAC}$ in 12 steps.

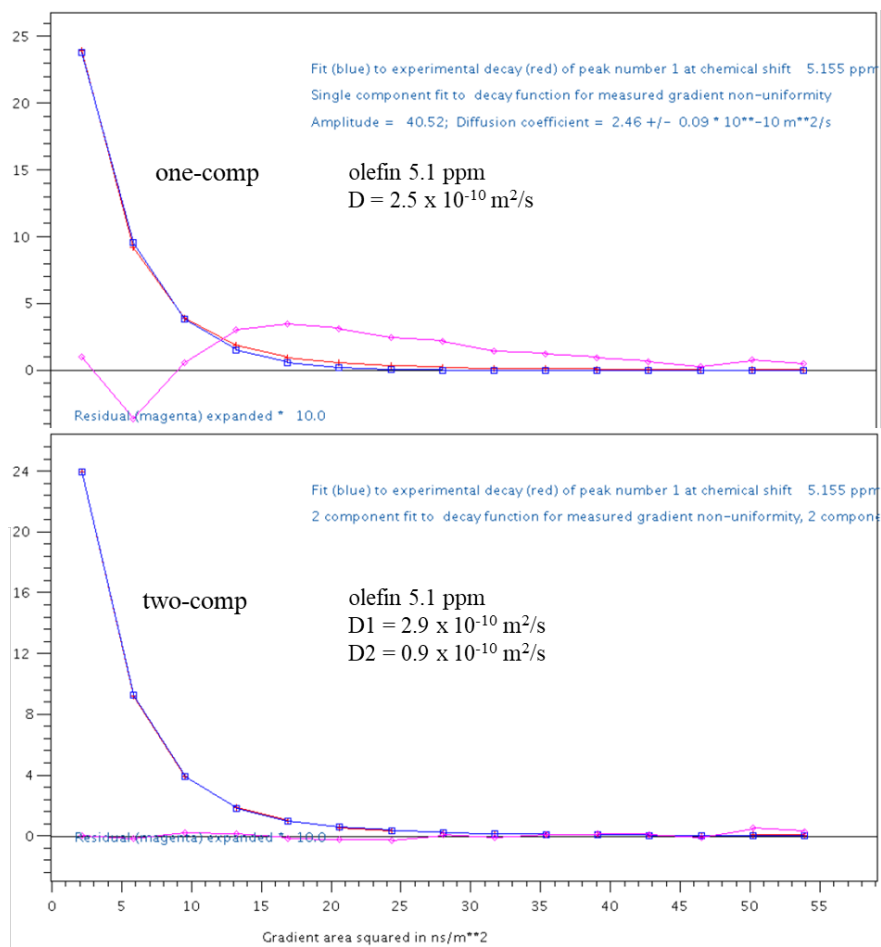


Figure S 9: Plot of echo intensity I (y axis) versus the gradient area squared $(\gamma G_z \delta)^2 ([?] - \delta/3)$ in ns^2/m^2 (x axis) in 1 and 2-component fits for the 5.1 ppm signal of thermally treated (210°C , 3h, air) methyl oleate collected with $\Delta = 140 \text{ ms}$, $\delta = 5 \text{ ms}$, $G = 5\text{-}25\text{k G/cm/DAC}$ in 15 steps.

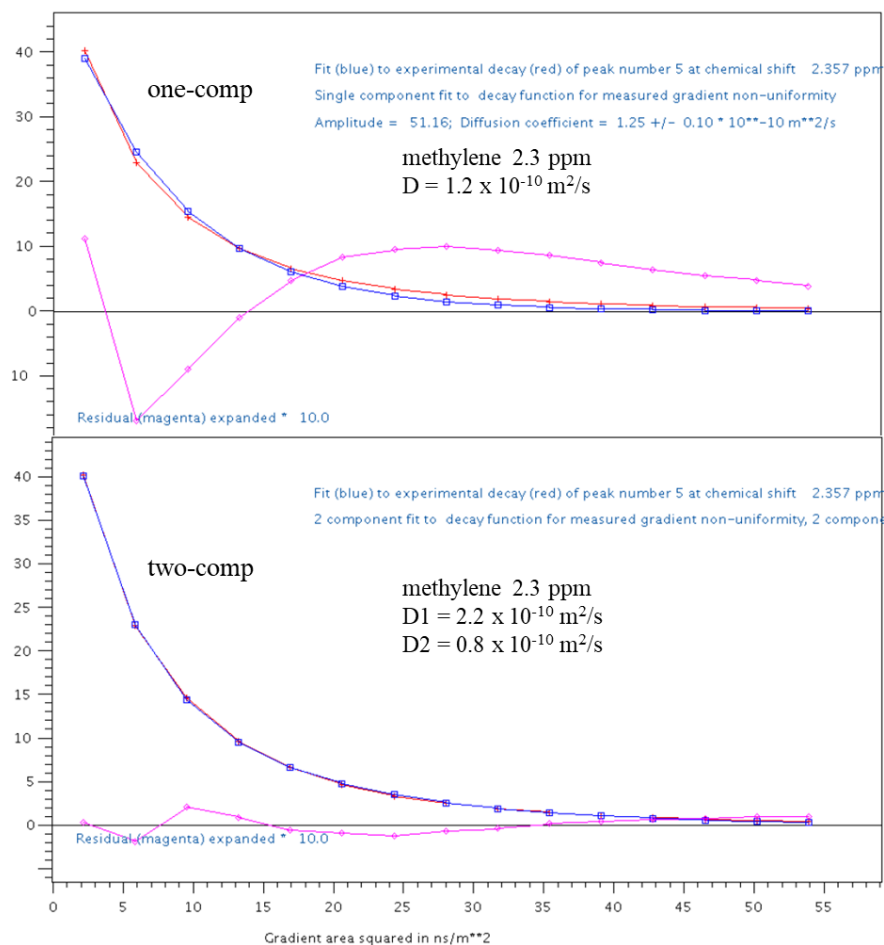


Figure S 9: Plot of echo intensity I (y axis) versus the gradient area squared $(\gamma G_z \delta)^2 ([?] - \delta/3)$ in ns/m² (x axis) in 1 and 2-component fits for the 2.3 ppm signal of thermally treated (210°C, 3h, air) methyl oleate collected with $\Delta = 140$ ms, $\delta = 5$ ms, $G = 5\text{-}25\text{k G/cm/DAC}$ in 15 steps.

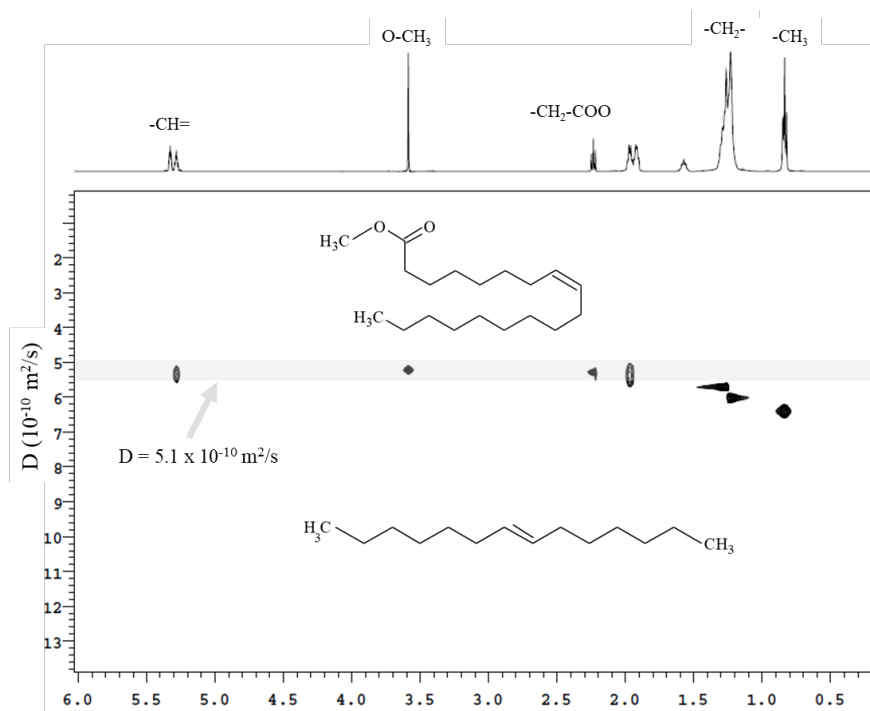


Figure S 10: DOSY plot of untreated methyl oleate mixed with trans-7-tetradecene dissolved in CDCl_3 collected with $\Delta = 140$ ms, $\delta = 5$ ms, $G = 5\text{-}10\text{k G/cm/DAC}$ in 12 steps.

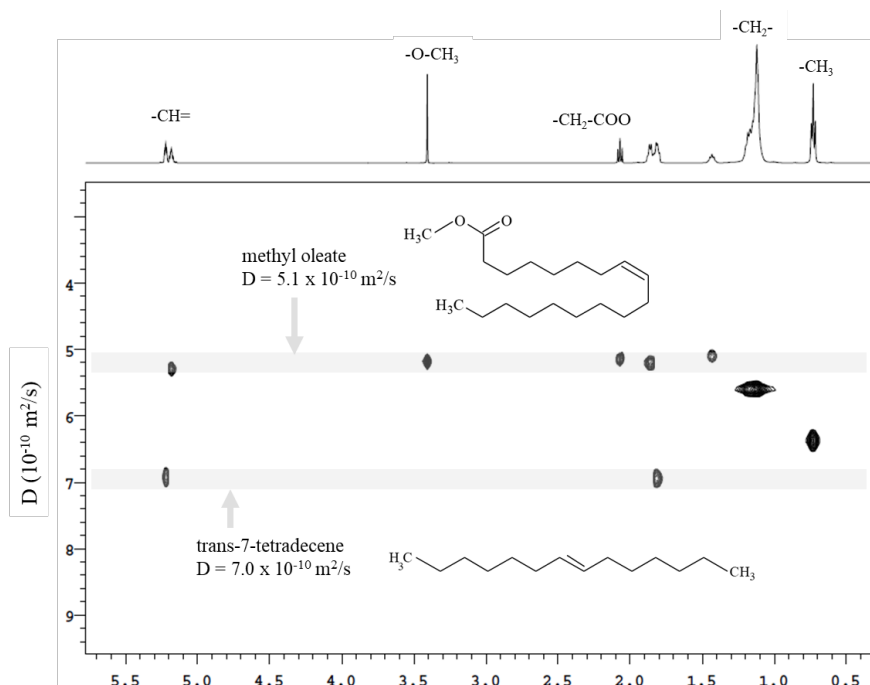


Figure S 11: DOSY plot of untreated methyl oleate mixed with trans-7-tetradecene dissolved in C_6D_6 collected with $\Delta = 140$ ms, $\delta = 5$ ms, $G = 5\text{-}10\text{k G/cm/DAC}$ in 12 steps.

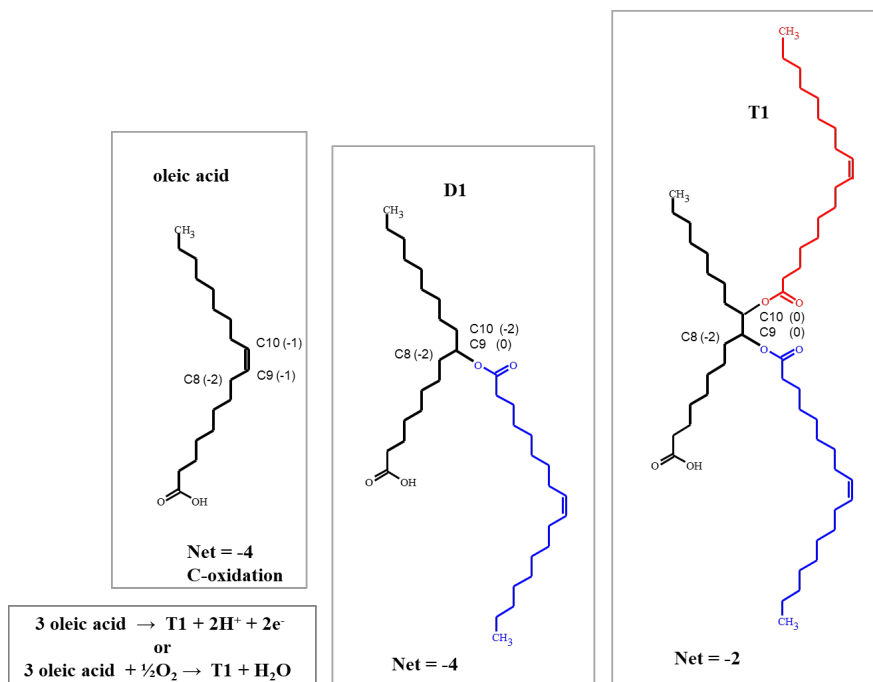


Figure S13. Net oxidation state for carbons 9 and 10 of oleic acid (-4) are unchanged on forming dimer (D1) with mono-addition of oxygen.

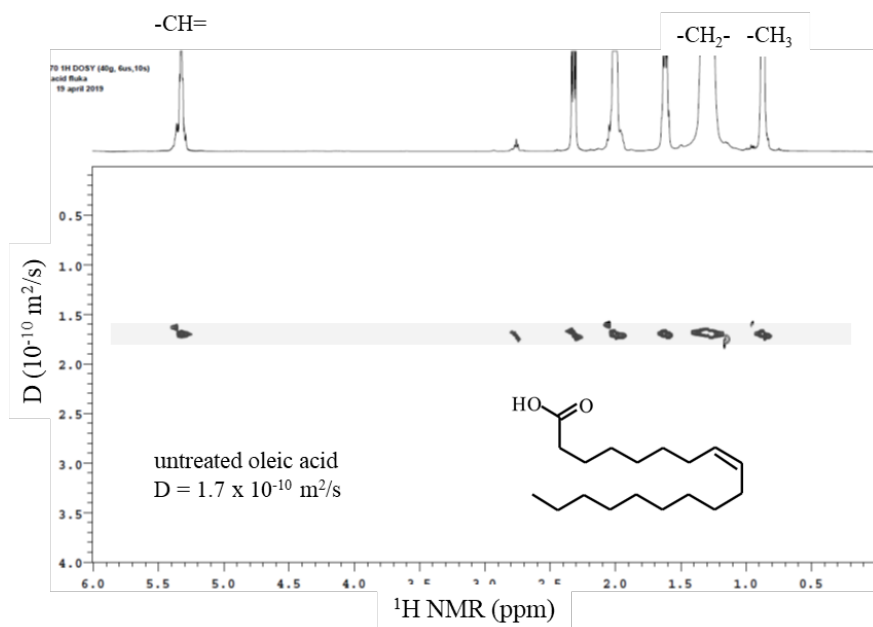


Figure S 12: DOSY plot of untreated oleic acid dissolved in CDCl₃ collected with $\Delta = 140$ ms, $\delta = 2$ ms, $G = 5\text{-}20\text{k G/cm/DAC}$ in 12 steps).

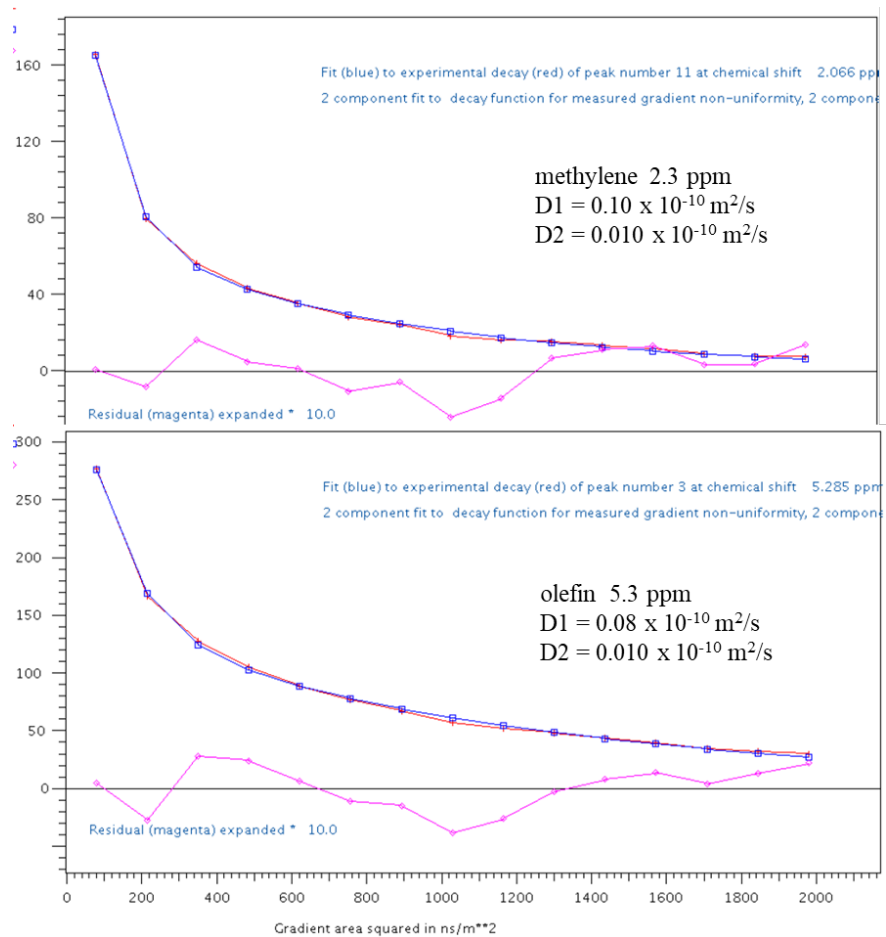


Figure S 13: Plot of echo intensity I (y axis) versus the gradient area squared $(\gamma G_z \delta)^2([\tau] - \delta/3)$ in ns/m^2 (x axis) in 2-component fits for the 2.0 ppm methylene signal (above) and 5.2 ppm olefin signal (below) of thermally treated (210°C , 3h, air) oleic acid collected with $\Delta = 90 \text{ ms}$, $\delta = 40 \text{ ms}$, $G = 5\text{-}25\text{k G}/\text{cm}/\text{DAC}$ in 15 steps.

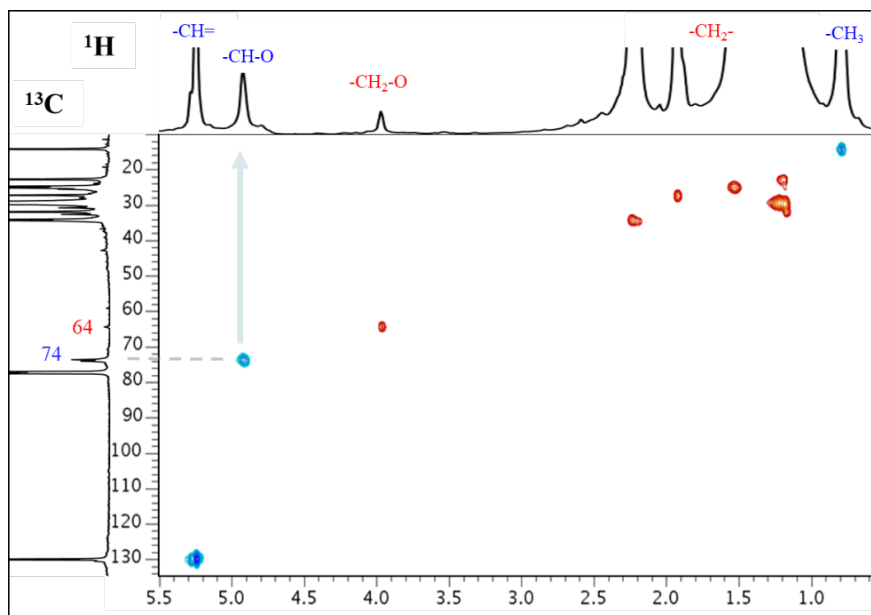


Figure S16. ^{13}C - ^1H HSQC NMR spectrum of oleic acid 210°C , 3h, air showing single-bond C-H correlations (CH_2 are red positive, CH and CH_3 are blue negative), e.g. ^{13}C signal at 64 ppm is due to a methylene carbon (attached to oxygen) with its hydrogens giving ^1H signal at 4.0 ppm.

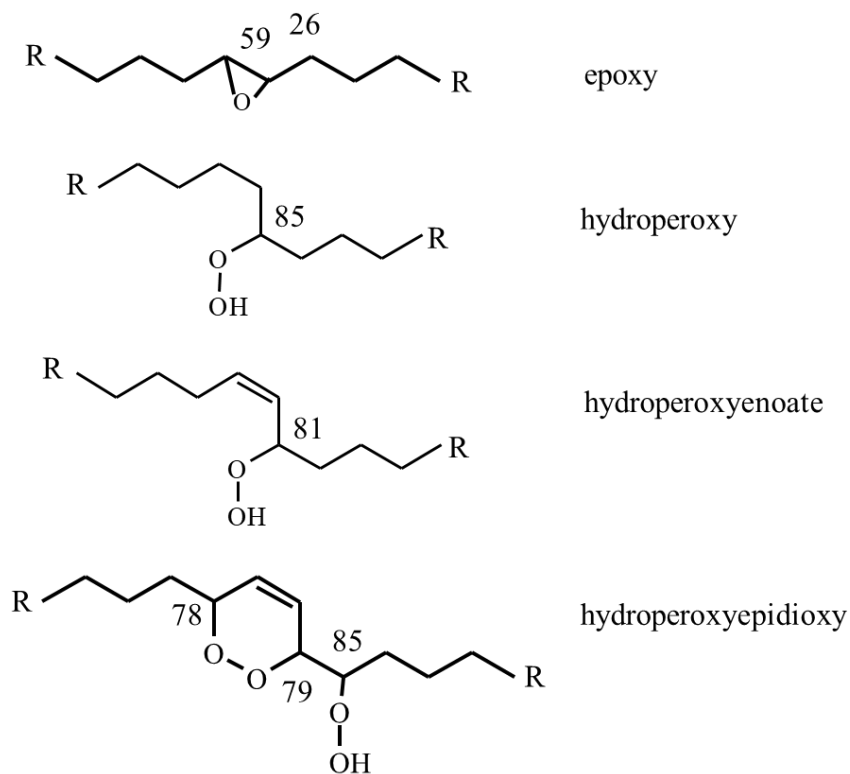


Figure S17. ^{13}C NMR shifts predicted (ACD) for oxidized species proposed by Alexandri et al. .

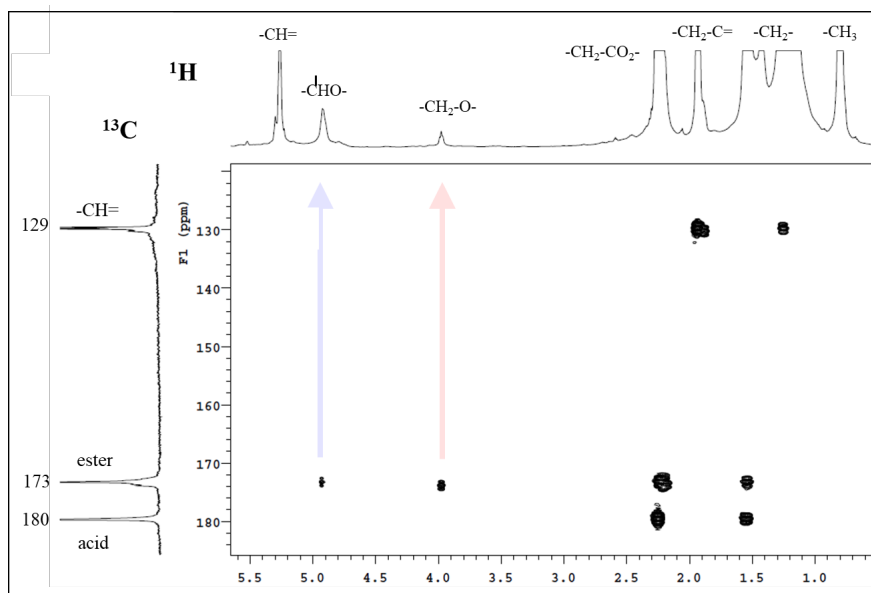


Figure S18. Expanded ^{13}C - ^1H HMBC NMR spectrum of oleic acid 210°C, 3h, air showing multiple-bond C-H correlations (over 3 covalent bonds). ^{13}C signal of ester carbon correlates with 4.9 ppm (methine-O) and 4.0 ppm (methylene-O) ^1H signals, while olefinic carbon shows no correlation with hydrogens of C-O carbons. Thus, carbons attached to oxygen are distant from olefinic carbon, ruling out alpha-hydroxyl olefins.

Long range ^{13}C - ^1H heteronuclear multiple bond correlations were made using Varian pulse program gHMB-CAD with 8 Hz multiple bond selection, one bond (130 to 165 Hz) suppression, 512 F1 increments and 16 scans. Carbons 3 covalent bonds away from a specific hydrogen are detected indirectly by quantum (scalar coupling) interactions ($J = 8$ Hz).

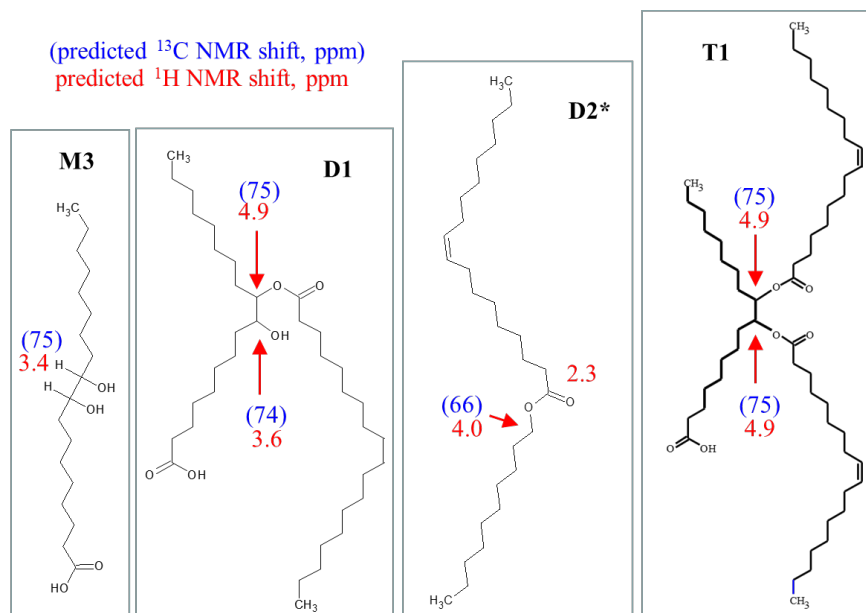


Figure S19. Simulated ^1H and (^{13}C) NMR shifts for selected carbons of oxidized monomer and dimers of oleic acid. Hydroxy ester D1 was not present since there is no CHO ^1H signal at 3.6 ppm. The signal observed at 4.0 ppm is from a CH_2O carbon.

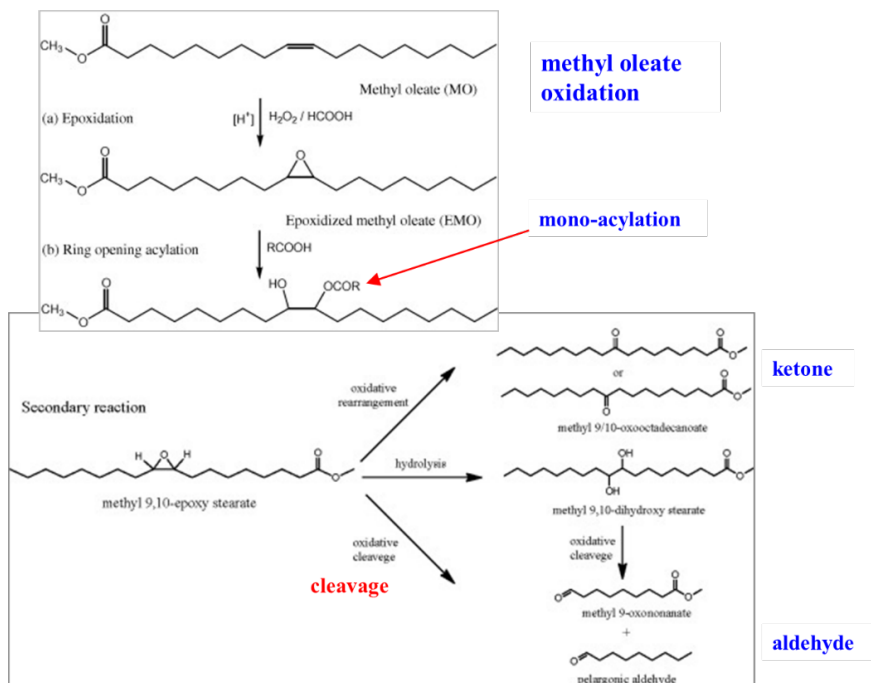


Figure S20: Oxidation of methyl oleate, with epoxidation and mono-acylation, primary reaction from Sharma et al. (top) and secondary reactions for methyl epoxy stearate with oxidative rearrangement, hydrolysis, or oxidative cleavage (bottom) from Seidensticker et al.).